European Journal of Medicinal Chemistry 83 (2014) 398–408

Contents lists available at ScienceDirect

European Journal of Medicinal Chemistry

journal homepage: http://www.elsevier.com/locate/ejmech

Original article

Novel 1-[4-(Aminosulfonyl)phenyl]-1*H*-1,2,4-triazole derivatives with remarkable selective COX-2 inhibition: Design, synthesis, molecular docking, anti-inflammatory and ulcerogenicity studies

Gamal El-Din A.A. Abuo-Rahma [a], Mohamed Abdel-Aziz [a, *], Nahla A. Farag [b], Tamer S. Kaoud [a, c]

[a] Medicinal Chemistry Department, Faculty of Pharmacy, Minia University, Minia 61519, Egypt
[b] Pharmaceutical Chemistry Department, Faculty of Pharmacy, Misr International University, Abbassia, 11566 Cairo, Egypt
[c] Division of Medicinal Chemistry, College of Pharmacy, The University of Texas at Austin, Austin, TX 78712, USA

ARTICLE INFO

Article history:
Received 15 February 2014
Received in revised form
8 June 2014
Accepted 24 June 2014
Available online 24 June 2014

Keywords:
1,2,4-Triazole
Anti-inflammatory
Ulcerogenicity
Cyclooxygenase selectivity
Docking study

ABSTRACT

A novel series of 1,2,4-triazole derivatives were synthesized and confirmed with different spectroscopic techniques. The prepared compounds exhibited remarkable anti-inflammatory activity comparable to that of indomethacin and celecoxib after 3 h. The tested compounds exhibited very low incidence of gastric ulceration compared to indomethacin. Most of the newly developed compounds showed excellent selectivity towards human COX-2 with selectivity indices (COX-1 IC_{50}/COX-2 IC_{50}) ranged from 62.5 to 2127. Docking studies results revealed that the highly selective tested compounds **6h** and **6j** showed lower CDOCKER energies, which means that they require less energy for proper interaction with the enzyme. The additional H-bonds with the oxygen of the amide and/or H of NH of the amide with the amino acid residues may be responsible for the higher binding affinity of this group of compounds towards COX-2.

1. Introduction

Non-steroidal anti-inflammatory drugs (NSAIDs) are considered one of the most useful clinical therapies for the treatment of pain, fever, and inflammation [1]. They exert their anti-inflammatory activity through inhibition of cyclooxygenase (COX) derived prostaglandin synthesis. Two isoforms of COX are found; COX-1 which is a housekeeping enzyme responsible for providing the physiological maintenance actions (vascular and renal homeostasis, gastroprotection) [2]. On the other hand, COX-2 isozyme which is induced by proinflammatory stimuli resulting in inflammatory actions [3]. Thus, selective inhibition of COX-2 is useful for the treatment of inflammations with reduced gastrointestinal toxicities [4,5]. The chronic use of NSAIDs, is associated with gastrointestinal [6–10], renal [11–13], and hepatic side effects [14] that are mainly due to inhibition of the beneficial COX-1 isozyme. Diaryl heterocycles have become the major class of selective COX-2 inhibitors, such as celecoxib, rofecoxib, parecoxib and valdecoxib (Fig. 1), which display improved gastrointestinal safety profile compared to the traditional NSAIDs [15–17]. In view of the gastric side-effects of conventional NSAIDs and the recent withdrawal of selective COX-2 inhibitors from the market due to their adverse cardiovascular side-effects, there is considerable impetus to develop alternative anti-inflammatory agents with reduced gastric and cardiovascular side effects [18]. Various 1,4- and 1,5-diaryl substituted 1,2,3-triazoles [19] (Fig. 2A) were evaluated as COX-2 inhibitors. From this study, it was concluded that compounds containing a vicinal diaryl substitution pattern display higher COX-2 inhibition potency compared to their corresponding 1,4-diaryl-substituted counterparts. 1,2,4-Triazol derivative [20] (Fig. 2B) exhibited a high in vitro COX-2 selectivity (COX-1 IC_{50} = 20.5 nM; COX-2 IC_{50} = 1.8 nM; SI = 11.39) relative to the reference drug celecoxib (COX-1 IC_{50} = 3.7 nM; COX-2 IC_{50} = 2.2 nM; SI = 1.68) and also showed good anti-inflammatory activity compared to celecoxib in a carrageenan-induced rat paw edema assay. A recent research study revealed that the presence of an additional ester group in the ortho-carbaboranyl analogues [21] with the small methyl ester group could further fine-tune the COX selectivity profile. Similarly, it was reported that the carboxyl moiety of acidic NSAIDs such as flurbiprofen interacts with Arg120 in both COX isoforms via hydrogen bonding or electrostatic interactions [22].

* Corresponding author.
E-mail addresses: abulnil@hotmail.com, abulnil2002@yahoo.com (M. Abdel-Aziz).

http://dx.doi.org/10.1016/j.ejmech.2014.06.049
0223-5234/

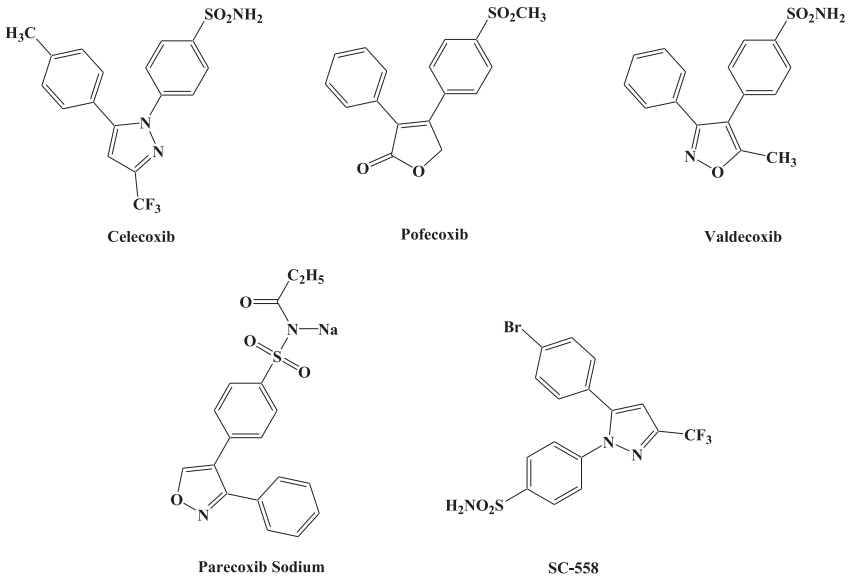

Fig. 1. Selective COX-2 inhibitors.

Promoted with the above-mentioned studies and as a continuation of our research interest [23–27] in the synthesis and biological evaluation of novel and safe NSAIDs; the present study is concerned with synthesis of novel 1-[4-(aminosulfonyl)phenyl]-1*H*-1,2,4-triazole derivatives containing triazole moiety as a bioisostere of the heterocyclic ring of the well known selective COX-2 inhibitors, keeping in mind the vicinal diaryl substituents with one having the 4-sulfamoyl group that fulfills the best pharmacophore for selective COX-2 inhibitors. In addition, the designed compounds contain an amide group, as a bioisostere for ester moiety, as an extra-binding site towards COX-2 that may enhance the selectivity. The prepared compounds are evaluated for their anti-inflammatory activity using carrageenan-induced rat paw edema and compared to the well-known NSAIDs, celecoxib and indomethacin. The ability of the prepared compounds to induce gastric toxicity and the selectivity to COX-1 and COX-2 isozymes has been also evaluated. Additionally, quantitative structure activity relationship (QSAR) studies were carried out for validation of the observed biological properties of the target compounds and for determination of the most important parameters controlling these properties. Moreover, docking studies were carried out using "Discovery studio software program". The scoring functions and hydrogen bonds formed with the surrounding amino acids are used to predict their binding modes, their binding affinities and orientation of these compounds at the active site of COX-2.

2. Results and discussion

2.1. Chemistry

The synthetic route used to prepare the target compounds **4, 5** and **6a–j** is outlined in Scheme 1. Heating of hippuric acid **1** with acetic anhydride afforded the intermediate **2**. The key intermediate **3** was prepared using Kuskov like reaction through coupling of the diazonium salt of sulfanilamide with the active methylene of **2** in presence of sodium acetate. Compounds **5** and **6a–j** were prepared via Sawdey rearrangement [28] of compound 3. Heating at reflux of **3** in methanolic potassium hydroxide afforded the methyl ester **4**. Hydrazinolysis of the ester **4** using hydrazine monohydrate (98%) in ethanol afforded the corresponding hydrazide **5** in a good yield. Moreover, reaction of the intermediate **3** with ammonia, or appropriate aliphatic amine including; isopropylamine, cyclohexylamine or benzylamine in methanol afforded the corresponding amides **6a–d**. Also, treatment of the intermediate **3** with the appropriate primary aromatic amines in acetic acid in presence of sodium acetate afforded the amides **6e–j**. The ^{1}H NMR of the amides **6a–j** showed the characteristic –NH signal at δ 10.74–9.29 ppm and the $-SO_2NH_2$ protons at δ 7.45–8.00 ppm. All the newly prepared compounds were identified using ^{1}H NMR, ^{13}C NMR and high resolution mass spectroscopy.

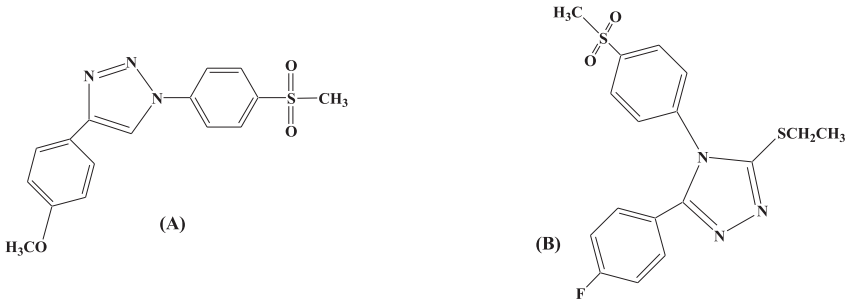

Fig. 2. 1,2,3-and 1,2,4-triazole derivatives as COX-2 inhibitors.

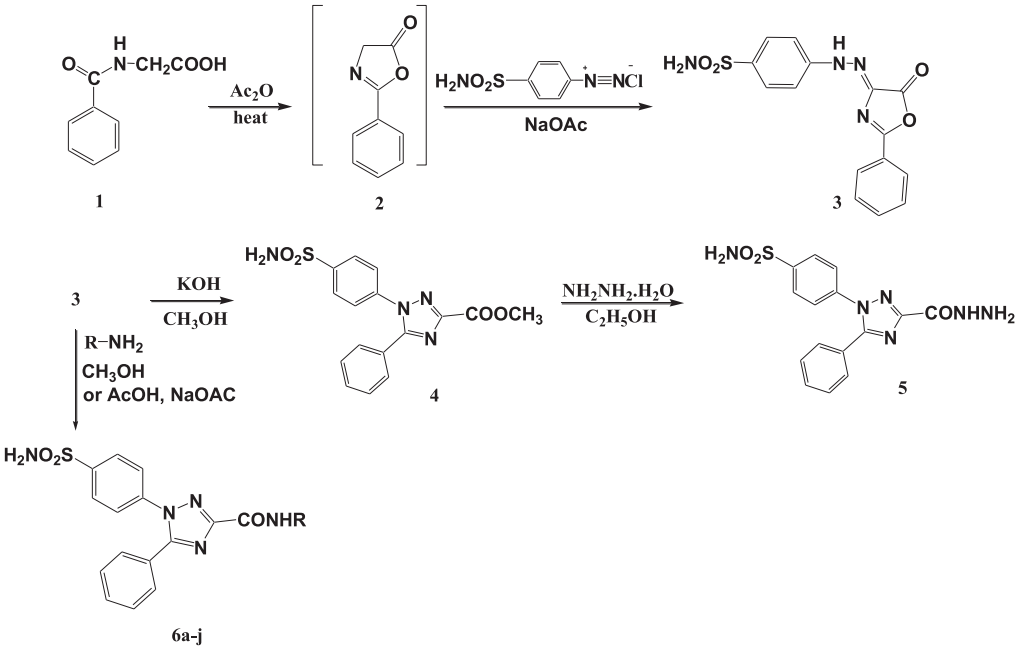

6a, R = H; **6b**, R = Isopropyl; **6c**, R = Cyclohexyl; **6d**, R = Benzyl; **6e**, R = 4-CH_3-Phenyl; **6f**, R = 4-OCH_3-Phenyl; **6g**, R = 3,4-Di-OCH_3-Phenyl; **6h**, R = 4-Cl-Phenyl; **6i**, R = 4-CH_3CO-Phenyl; **6j**, R = 2-Benzothiazolyl.

Scheme 1. Synthesis of the target compounds **4**, **5** and **6a**–**j**.

2.2. Biological investigations

2.2.1. Screening of anti-inflammatory activity

The synthesized compounds **4**, **5** and **6a**–**j** were evaluated for their anti-inflammatory activity using carrageenan-induced paw edema method in rats described by Winter *et* al. [29] The test compounds and the reference drugs indomethacin and celecoxib were administered orally at a dose level of 0.28 mmol/kg; 30 min before carrageenan injection at the right hind paw of Albino male rats. The thickness of both paws was measured at different times of 1, 2, 3, 4 and 5 h after carrageenan injection. The anti-inflammatory activity of the tested compounds, celecoxib and indomethacin was calculated as the percentage decrease in edema thickness induced by carrageenan and was determined using the following formula:

$$\%\ \text{of edema inhibition} = \frac{(V_R - V_L)_{\text{control}} - (V_R - V_L)_{\text{treated}}}{(V_R - V_L)_{\text{control}}}$$

Where V_R represents the mean right paw thickness and V_L represents the mean left paw thickness.

Table 1
The anti-inflammatory activity at different times and ulcer indices of compounds **4**, **5** and **6a**–**j** compared to **celecoxib** and **indomethacin**.

Compound	% Of edema inhibition (% mean ± S.E.M)				
	1 h	2 h	3 h	4 h	5 h
Control	0	0	0	0	0
4	38.00 ± 1.80***	48.00 ± 1.32***	69.00 ± 1.44***	61.00 ± 1.20***	46.00 ± 1.00***
5	32.00 ± 1.60***	53.00 ± 1.27***	60.00 ± 1.10***	45.00 ± 1.70***	32.00 ± 2.00***
6a	43.00 ± 1.00***	48.00 ± 1.00***	52.00 ± 1.40***	49.00 ± 0.94***	42.00 ± 1.32***
6b	21.00 ± 1.46***	43.00 ± 2.00***	55.00 ± 1.70***	44.00 ± 0.70***	43.00 ± 1.80***
6c	20.00 ± 2.38***	43.00 ± 1.20***	65.00 ± 1.31***	53.00 ± 1.28***	42.00 ± 2.61***
6d	42.00 ± 1.30***	47.00 ± 2.00***	58.00 ± 2.00***	36.00 ± 1.60***	29.00 ± 0.90***
6e	40.00 ± 1.55***	47.00 ± 2.00***	76.00 ± 1.00***	71.00 ± 2.70***	65.00 ± 2.00***
6f	53.00 ± 1.18***	57.00 ± 2.42***	78.00 ± 1.31***	73.00 ± 1.30***	55.00 ± 1.40***
6g	22.00 ± 1.21***	52.00 ± 1.26***	72.00 ± 1.00***	63.00 ± 1.93***	60.00 ± 1.16***
6h	36.00 ± 1.31***	62.00 ± 2.00***	67.00 ± 2.00***	53.00 ± 2.20***	44.00 ± 1.09***
6i	53.00 ± 1.12***	68.00 ± 1.33***	73.00 ± 2.47***	64.00 ± 1.30***	42.00 ± 0.78***
6j	20.00 ± 1.16***	32.00 ± 1.40***	54.00 ± 1.50***	44.00 ± 1.77***	38.00 ± 1.20***
Celecoxib	44.00 ± 1.00***	50.00 ± 1.25***	69.00 ± 1.30***	59.00 ± 2.00***	52.00 ± 2.09***
Indomethacin	54.00 ± 0.81***	66.00 ± 2.00***	79.00 ± 1.17***	81.00 ± 2.39***	84.00 ± 1.87***

*** Significantly different from control group at $P < 0.001$.
Note. *one way* ANOVA test was applied to determine the significance of the difference between the control group and rats treated with the tested compounds. ($n = 4$), ***$p < 0.001$, significant difference from control group.

$(V_R - V_L)_{control}$ represents the mean increase in paw thickness in the control group of rats.

$(V_R - V_L)_{treated}$ represents the mean increase in paw thickness in rats treated with the test compounds.

The results listed in Table 1 show the percentage of edema inhibition induced by carrageenan for the tested compounds, celecoxibs and indomethacin versus time in h. The obtained results indicated that most of the test compounds revealed significant ($p < 0.001$) inhibition against carrageenan-induced paw edema in rats and the maximum anti-inflammatory activity was obtained after 3 h. Then, the activity decreased gradually for the next 2 h. Indomethacin showed an inhibitory activity of 79% while celecoxib exhibited an inhibitory activity of 69% against carrageenan-induced paw edema after 3 h. Compounds **6f**, **6e, 6i** and **6g** exhibited good anti-inflammatory activity of 78%, 76%, 73% and 72%, respectively, which represents 99%, 96%, 92% and 91% of indomethacin activity and 113%, 110%, 106% and 104% of celecoxib activity, respectively, after 3 h (Table 2). The ester **4** exhibited moderate anti-inflammatory activity of 69% against carrageenan-induced paw edema after 3 h; that represents 87% and 100% of indomethacin and celecoxib activities, respectively. The anilides **6h** and **6c** showed remarkable anti-inflammatory activities of 67% and 65% against carrageenan-induced paw edema after 3 h; that represents 85% and 82% of indomethacin and 97% and 94% of celecoxib activities, respectively. The remaining anilides showed a variable anti-inflammatory activity ranging from 52% to 62% that represent from 66% to 76% of indomethacin and 75%–87% of celecoxib activities, respectively (Tables 1 and 2). The aforementioned results indicated that substitution on the amide nitrogen by an aromatic moiety e.g. 4-methoxyphenyl (**6f**), 4-methylphenyl (**6e**), 4-acetylphenyl (**6i**) 3,4-dimethoxyphenyl (**6g**), and 4-chlorophenyl (**6h**) is associated with increasing of the anti-inflammatory activity compared to substitution on the amide nitrogen by an aliphatic moiety e.g. cyclohexyl (**6c**), isopropyl (**6b**), the unsubstituted amide (**6a**) and the hydrazide (**5**). The results in Table 1 also indicated that the substitution on the amide nitrogen by a *p*-substituted phenyl with electron donating groups such as CH_3 or OCH_3 (**6f** and **6e**) is associated with increasing the anti-inflammatory activities of these compounds compared with similar derivatives with electron withdrawing moiety such as $-COCH_3$, –Cl and -benzothiazol **6i**, **6h** and **6j**, respectively. Additionally, the presence of only one 4-methoxy (**6f**) is associated with a little increase of the anti-inflammatory activity compared to the presence of 3,4-dimethoxy moieties (**6g**).

Table 2
% Activity and ulcer indices of the tested compounds **4**, **5** and **6a**–**j** relative to **celecoxib** and **indomethacin**.

Compound	% Activity relative to indomethacin after 3 h	% Activity relative to celecoxib after 3 h	UI mean ± S.E.M
Control	0	0	0.0 ± 0.00
4	87	100	3.0 ± 0.40***
5	76	87	3.0 ± 0.70***
6a	66	75	2.0 ± 0.33**
6b	70	80	0.0 ± 0.0***
6c	82	94	0.0 ± 0.0***
6d	73	84	3.0 ± 0.60**
6e	96	110	1.0 ± 0.33**
6f	99	113	2.3 ± 0.18**
6g	91	104	0.0 ± 0.0***
6h	85	97	0.5 ± 0.11***
6i	92	106	0.5 ± 0.23**
6j	68	78	1.0 ± 0.25***
Celecoxib		100	0.5 ± 0.40***
Indomethacin	100		39.0 ± 0.60***

** Significantly different from control group at $P < 0.01$.
*** Significantly different from control group at $P < 0.001$.
Note. *one way* ANOVA test was applied to determine the significance of the difference between the control group and rats treated with the tested compounds. ($n = 4$), $^{**}p < 0.01$, $^{***}p < 0.001$, significant difference from control group.

2.2.2. Screening of ulcerogenicity

The *in vivo* ulcerogenic liability was evaluated for the synthesized compounds **4**, **5** and **6a**–**j** relative to both celecoxib and indomethacin according to a reported procedure [30]. Ulcers were classified into levels, level I, ulcer areas less than 1 mm^2, level II, ulcer areas from 1 to 3 mm^2 and level III, ulcer areas more than 3 mm^2, and the ulcer index (UI) was calculated as follows:

$$\begin{aligned} UI = {} & 1 \times (\text{number of ulcers level I}) \\ & + 2 \times (\text{number of ulcers level II}) \\ & + 3 \times (\text{number of ulcers level III}),\ \text{etc.....} \end{aligned}$$

The UIs of compounds **4**, **5** and **6a**–**j** were calculated and listed in Table 2 as (mean ± S.E.M). The results of ulcerogenic liability revealed that indomethacin caused significant ulcerogenic toxicity with UI of **39**, while celecoxib exhibited very low UI of 0.5. All of the synthesized compounds exhibited very lower UIs compared to indomethacin. Compounds **4** and **5** exhibited lower ulcerogenic liability relative to indomethacin with UI of 3 (Fig. 3A and B). Meanwhile, the anilides **6a**–**j** exhibited very low gastric toxicity compared to indomethacin with UI ranging from zero to 3 (Fig. 3A and B). The obtained results revealed that all of the tested compounds exhibit safer ulcerogenic liability relative to indomethacin and comparable to that of celecoxib.

2.3. Selectivity to COX-1 and COX-2

The effects of compounds **6b**–**h** and **6j** on the activity of ovine COX-1 (using SC-560 as a reference [31,32]) and on human recombinant COX-2 using (DuP-697 as a reference [33]) were

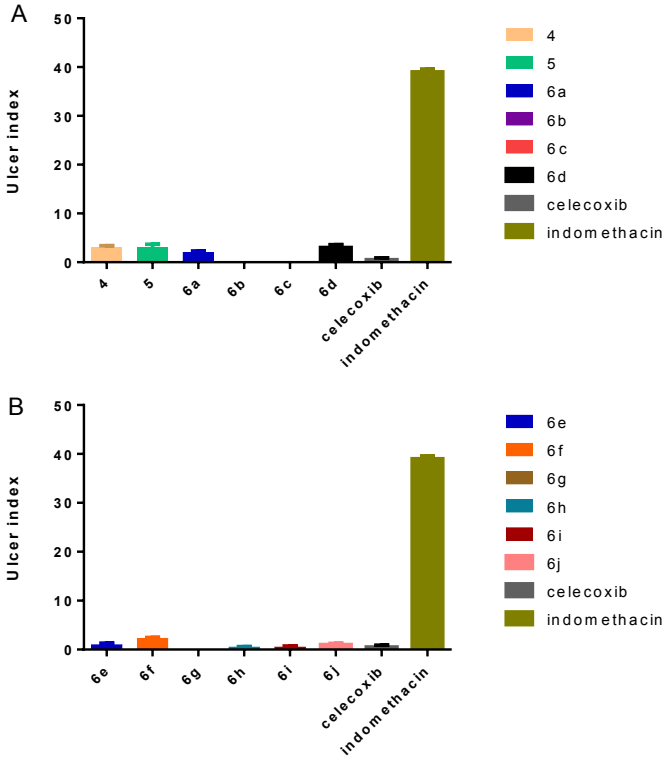

Fig. 3. A. UI of compounds **4, 5** and **6a**–**d** compared to indomethacin and celecoxib expressed as mean ± S.E.M. **B**. UI of compounds **6e**–**j** compared to indomethacin and celecoxib expressed as mean ± S.E.M.

estimated using fluorescent inhibitor screening assay kit (Cayman Chemical, Ann Arbor, MI, USA). The dose response curves (Fig. 4A–H) and IC_{50} values (Table 3) were determined for each compound. Unlike indomethacin (COX-1 selective inhibitor), the newly developed compounds exhibited remarkable selectivity towards human COX-2 if compared to ovine COX-1 (Fig. 4). The in vitro COX-2 selectivity indices are ranging from 62.5 to 2127 (Table 3) for compounds **6b**, **6c**, **6d**, **6e**, **6f**, **6g**, **6h** and **6j** while it was reported to be 0.004 for indomethacin [34,35] and 600 for celecoxib (COX-2 selective inhibitor) [36]. It is obvious that there is no remarkable effect on the selectivity index upon changing the substitution on the amide nitrogen by an aliphatic or aromatic moiety. The *N*-cyclohexyl **6c** and *N*-benzyl **6d** derivatives exhibited lower selectivity index compared to *N*-isopropyl derivative **6b**. Additionally, substitution on the amide nitrogen by a *p*-chlorophenyl or 2-benzothiazolyl moieties revealed the best selectivity indices compared to other derivatives.

Table 3
In vitro COX-1 and COX-2 enzyme inhibition data for compounds **6b**–**h** and **6j** compared to **indomethacin**, **celecoxib**, **SC-560** and **DuP-697**.

Compound	COX-1 IC_{50} (μM)[a]	COX-2 IC_{50} (μM)[a]	SI[b]
6b	>1000	16 ± 2.00	62.50
6c	>1000	0.66 ± 0.120	1515
6d	>1000	1.7 ± 0.180	588
6e	516 ± 74.0	1.9 ± 0.140	271
6f	>1000	0.89 ± 0.200	1123
6g	346 ± 15.0	1.3 ± 0.150	266
6h	>1000	0.47 ± 0.021	2127
6j	798 ± 100	0.38 ± 0.050	2100

[a] The in vitro test compound concentration required to produce 50% inhibition of either COX-1 or COX-2 activity, calculated from the dose response curve of inhibition. The result (IC_{50}, μM) is the mean of three determinations acquired using the COX Inhibitor Screening Assay Kit (Catalog No. 560131, Cayman Chemicals Inc., Ann Arbor, MI, USA).
[b] In vitro COX-2 selectivity index (COX-1 IC_{50}/COX-2 IC_{50}).

2.4. Docking studies

2.4.1. QSAR modeling

The 2D structures of the training set analogs were imported into the Discovery Studio to calculate various molecular descriptors for compounds **6b**–**h** and **6j**. The 2D molecular descriptors such as AlogP, molecular properties, molecular property counts, and surface area volume were used as input molecular properties that could describe the molecules [37]. MLR technique was used in the present study for selecting a significant set of descriptors in order to

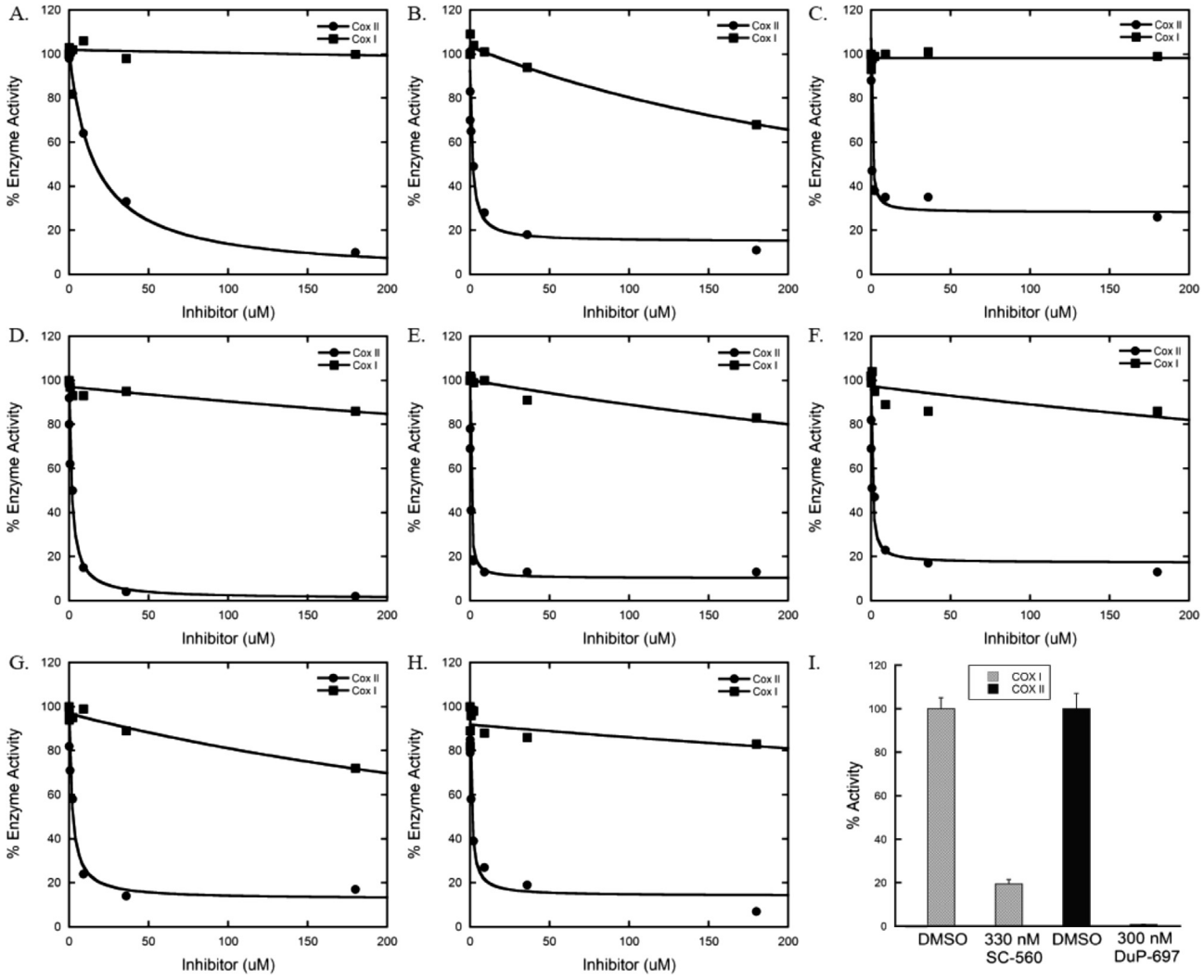

Fig. 4. A–**H**. The effects of compounds **6b** (A), **6c** (B), **6d** (C), **6e** (D), **6f** (E), **6g** (F), **6h** (G) and **6j** (H) on the activity of ovine COX-1 (■) and human recombinant COX-2 (●). Inhibition of ovine COX-1 by 330 nM SC-560 and human recombinant COX-2 by 300 nM DuP-697 (I). The results are expressed as percent of control in the absence of inhibitor (100% maximum activity).

build the significant models. Equation 1 represents the best performing QSAR models (Fig. 5) show the corresponding scatter plots of the experimental versus estimated bioactivity values for the training set compounds as COX-2 inhibitor. The MLRTempModel equation bearing the relevant descriptors is given as follow:

$$-\text{LogIC50} = -0.622161\,\text{ALog}P - 0.0135553\,\text{Molecular Weight} - 0.436435\,\text{Num Aromatic Rings} + 0.269189\,\text{Num H Acceptors} + 1.45282\text{Num Rings} - 0.0364895\,\text{Num Rotatable Bonds} - 0.0493985\,\text{Molecular Fractional Polar Surface Area} - 0.0440254.$$

Where ALog*P* is a measure of the hydrophobicity of the molecule; it is calculated in Discovery Studio as the Log of the octanol–water partition coefficient.

Molecular Fractional Polar Surface Area is the ratio of the polar surface area divided by the total surface area of the molecule.

$-\text{logIC50}$: (the negative logarithmic value of the concentration required to produce 50% inhibition of COX −2 enzyme compared to the control experiment).

The method used to build the model was Least-Squares.

($N = 7$, $r^2 = 1.000$, r^2 adjusted = 1.000, r^2 prediction = 1.000), where **r^2 (adj)** is r^2 adjusted for the number of terms in the model; **r^2 (pred)** is the prediction r^2, equivalent to q^2 from a leave-1-out cross-validation. Number of hydrogen donor descriptor was excluded from the model for being constant. Where, it shows the direct relationship of hydrogen acceptor count, and number of rings descriptors reveals their importance for selective potent molecule design.

2.4.2. Validation of QSAR

External validation of the determined QSAR models was performed utilizing the synthesized analogs **6b**–**h** and **6j**.

It should be noted that the predicted anti-inflammatory activities by QSAR models were very close to those experimentally observed, where predicted IC_{50} of **6h** (use identified as statistical outlier) is 0.31 μM and its experimental IC_{50} is 0.47 μM, indicating that these models can be safely applied for predication of more effective hits having the same skeletal framework as that of the potent selective COX-2 inhibitor compounds.

Table 4
CDocker energy interaction, amino acid residues which form hydrogen bonds, IC_{50} COX-2 in μM and length of hydrogen bond (A) with ligand for compounds **6a**–**j** compared to **SC-558**.

Compound	-(CDocker energy interaction)	Amino acid residues which form hydrogen bonds with ligand	IC_{50} COX-2 in μM	Length of hydrogen bond (A)
SC-558	49.0774	Arg120 H–F of CF_3		2.12
		Arg 513 H–O of SO_2NH_2		2.02
		Ser 353 O–NH of SO_2NH_2		2.07
6a	**40.6659**	Arg 120 H–O of SO_2NH_2	NA	2.02
		Arg 315 H–O of $CONH_2$		2.24
6b	**53.1608**	Arg 120 H–O of SO_2NH_2	16 ± 2	2.49
6c	**44.2243**	Arg 513 H–O of SO_2NH_2	0.66 ± 0.12	1.82
		Ser 353 O–H of SO_2NH_2		2.13
		Leu 352 O–H of SO_2NH_2		2.36
6d	**36.9765**	Leu 352 O–H of CONH	1.7 ± 0.18	2.43
6e	**38.0162**	Arg 120 H–N of SO_2NH_2	1.9 ± 0.14	2.47
6f	**41.1984**	Leu 352 O–H of CONH	0.89 ± 0.2	2.38
6g	**23.9268**	Arg 120 H–N of SO_2NH_2	1.3 ± 0.15	1.93
		Arg 120 H–O of SO_2NH_2		2.38
		Arg 513 H–O of SO_2NH_2		2.00
		Glu 524 O–H of SO_2NH_2		2.09
		Glu 524 O–H of SO_2NH_2		2.06
6h	**30.7184**	His 90 N–H of CONH	0.47 ± 0.021	2.35
		Ser 353 O–H of CONH		2.25
6i	**41.0442**	Leu 352 H of NH–O of SO_2NH_2	NA	1.98
		Gln 192 H–O of SO_2NH_2		2.33
6j	**47.0161**	Arg 120 H–O of SO_2NH_2	0.38 ± 0.05	2.42
		Arg 513 H–O of CONH		2.46
		Gln 192 H–N of benzothiazole		2.42
		Leu 352 O–H of CONH		1.87

2.4.3. Docking analysis

To predict the anti-inflammatory data on a structural basis, automated docking studies were carried out using Discovery studio software program [37]. The scoring functions and hydrogen bonds formed with the surrounding amino acids are used to predict their binding modes, their binding affinities and orientation of these compounds at the active site of the COX-2 enzyme. The protein-ligand complex was constructed based on the X ray structure of COX-2 (prostaglandin-endoperoxide synthase 2) complex with a selective inhibitor **SC-558** available through the RCSB Protein Data Bank (PDB entry 1CX2) [38]. The scoring functions of the compounds were calculated from minimized ligand protein complexes. In order to compare the binding affinity of the newly synthesized derivatives, compounds **6a**–**j** were docked into the empty binding site of COX-2 (1CX2) and the results are listed in Table 4. **SC-558**

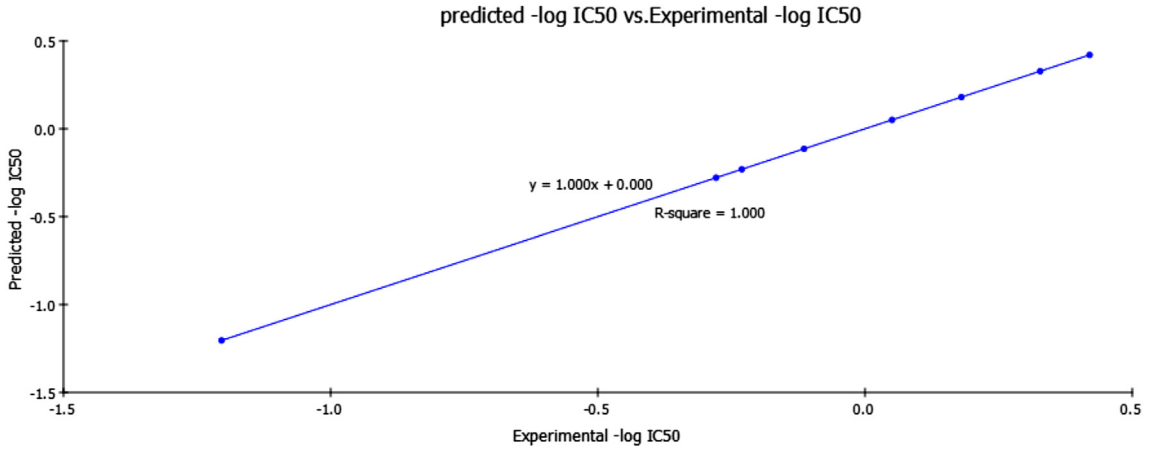

Fig. 5. Predicted versus experimental-log IC_{50} of the tested compounds as COX-2 inhibitors.

(the original ligand) revealed CDOCKER interaction energy of −49.08 and forms three hydrogen bonds with Arg-120, Arg-513 and Ser-353 (Table 4). Compound **6j** exhibited the highest inhibitory activity with IC_{50} of 0.38 revealed scoring value of −47.02 and forms four hydrogen bonds with Arg-120, Arg-513, Gln-192, and Leu-352 (Table 4, Fig. 6). Compound **6h** of IC_{50} of 0.47 exhibited scoring value of −30.72 and form two hydrogen bonds with His-90, and Ser-353 (Table 4, Fig. 7). From the obtained results in Table 4, Figs. 6 and 7 it is obvious that the highly selective COX-2 (compounds **6j** and **6h**) showed lower CDOCKER energies, which means that they require less energy for proper interaction with the receptor. Also it was found that compounds **6a, 6d, 6f, 6h and 6j** form additional H-bonds with the oxygen of the amide and/or H of NH of the amide with the amino acid residues which may lead to higher binding affinity with the enzyme and accordingly higher inhibition ability. Additionally, all of the docked compounds exhibit Pi cation interaction between aromatic phenyl of benzene sulfonamido and/or triazole moieties with the cation of Arg-120 resulting in high binding affinity and hence high inhibitory activity for COX-2 enzyme.

3. Conclusion

A series of novel 1,2,4-triazole derivatives was prepared and confirmed with different spectroscopic techniques. Most of the synthesized compounds showed significant anti-inflammatory activity with low incidence of gastric ulceration comparable to that of indomethacin and celecoxib. Most of the newly developed compounds showed excellent selectivity towards human COX-2 compared to COX-1. The remarkable binding affinity to COX-2 enzyme may be attributed to the formation of additional H-bonds with the oxygen of the amide and/or H of NH of the amide with the amino acid residues of the enzyme. Additionally, all of the docked compounds exhibit Pi cation interaction between aromatic phenyl of benzene sulfonamido and/or triazole moieties with the cation of Arg-120 resulting in high binding affinity and consequently high inhibitory activity for COX-2 enzyme. In summary, the introduction of this novel 1,2,4-triazole derivatives with additional binding moieties to COX-2 looks a promising approach to improve the safety of NSAIDs and may be a challenge in the field of COX-2 inhibitory therapy.

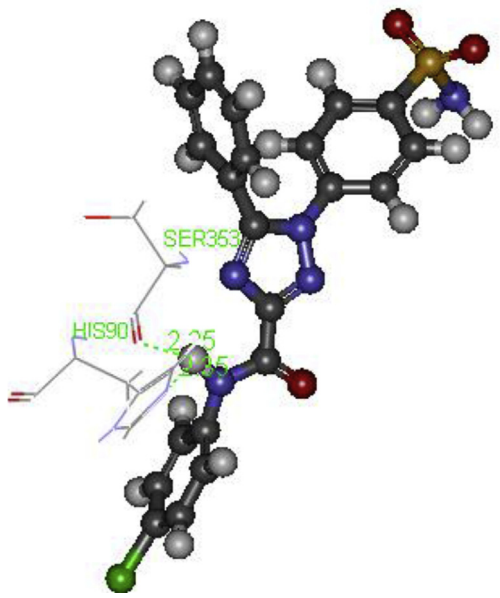

Fig. 6. Binding mode of compound **6h** in the binding site of COX-2 (for interpretation of the references to color in the text, the reader is referred to the web version of this article).

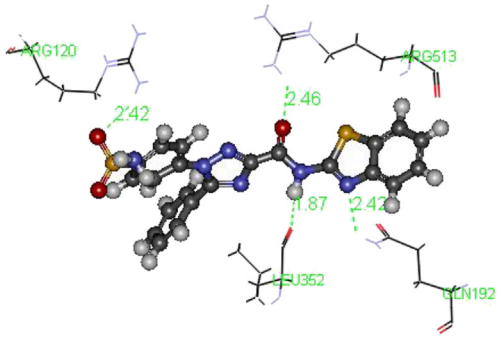

Fig. 7. Binding mode of compound **6j** in the binding site of COX-2 (for interpretation of the references to color in the text, the reader is referred to the web version of this article).

4. Experimental section

Reactions were monitored by TLC: Pre-coated plastic sheets, 0.2 mm silica gel with fluorescent indicator (Macherey–Nagel). Melting points were determined on Stuart electrothermal melting point apparatus and were uncorrected. IR spectra were recorded on Nicolet iS5 (ATR) FT-IR spectrometer. ^{1}H NMR spectra were recorded using a 400 MHz Bruker AM 400 spectrometer and Bruker Advance 400 and 300 MHz NMR spectrometer. ^{13}C NMR spectra were recorded using 100 MHz Bruker AM 400 spectrometer and Bruker Advance (75 MHR) spectrometer. Chemical shifts δ values are given in parts per million (ppm) using $CDCl_3$ (7.29 for proton and 76.98 for carbon), DMSO-d_6 (2.5) as solvents and coupling constants (J) in Hertz. Splitting patterns are designated as follows: s, singlet; d, doublet; t, triplet; q, quartet; dd, doublet of doublet; m, multiplet; bs, broad singlet instrument. High resolution mass spectra (HRESIMS) were obtained on Thermo Scientific Q Exactive Orbitrap LC-MS/MS System and were reported as mass/charge (m/z) with percent relative abundance.

4.1. Chemistry

4.1.1. 4-[2-(5-Oxo-2-phenyl-4,5-dihydro-1,3-oxazol-4-yliden) hydrazino]-1-benzenesulfonamide **3**

Hippuric acid 1 (11.5 g, 0.065 mol) in acetic anhydride (40 mL) was heated to 80 °C until a clear solution of the intermediate **2** was obtained. The resulting solution was cooled to room temperature (Solution A). To a cold solution of sulphanilamide (8.6 g, 0.05 mol) in 5 M HCl (17.5 mL) in an ice bath (0–5 °C), a solution of sodium nitrite (4.48 g, 0.065 mol) in water (10 ml) was added in a dropwise manner. The reaction mixture was left for 15 min (Solution B). Solution A was added to solution B in presence of anhydrous sodium acetate (7.5 g, 0.09 mol). The reaction mixture was stirred at (0–5 °C) for 4 h, the formed precipitate was filtered off and dried. The product was obtained as orange powder; mp: 236–237 °C; Yield = 16.57 g, 75.00%; ^{1}H NMR (400 MHz, DMSO-d_6) δ 10.70 (s, 1H, NH), 8.80–9.00 (m, 2H, $-SO_2NH_2$), 7.20–7.60 (m, 3H, Ar–H), 7.70 (d, 2H, J = 7.80 Hz, Ar–H), 7.85 (d, 2H, J = 7.80 Hz, Ar–H), 7.86–7.90 (m, 1H, Ar–H), 8.18 (d, 1H, J = 7.80 Hz, Ar–H); ^{13}C NMR (100 MHz, DMSO-d_6) 171.29, 166.45, 162.56, 161.16, 145.30, 138.23, 133.96, 133.76, 131.40, 129.38, 126.67, 114.49.

4.1.2. Methyl 1-[4-(aminosulfonyl)phenyl]-5-phenyl-1H-1,2,4-triazole-3-carboxylate **4**

To a stirred suspension of **3** (3.44 g, 0.01 mol) in methanol (30 mL), potassium hydroxide (5%, 5 mL) was added, with continuous stirring for 1 h at room temperature. The solvent was evaporated under reduced pressure; the formed precipitate was filtered, dried and recrystallized from methanol affording compound **4** as orange powder; mp: 218–220 °C Yield = 2.33 g, 65%; FT-IR (cm^{-1}): 3352, 3212, 1751, 1596, 1563; ^{1}H NMR (400 MHz, DMSO-d_6) δ 7.90 (d, 2H, J = 8.00 Hz, Ar–H) 7.58–7.48 (m, 4H, Ar–H + $-SO_2NH_2$), 7.44–7.38 (m, 3H, Ar–H); 7.34–7.27 (m, 2H, Ar–H), 3.90 (s, 3H, $-CH_3$); ^{13}C NMR (100 MHz, DMSO-d_6) 159.77, 155.38, 153.70, 144.87, 139.67, 133.93, 130.79, 129.05, 128.81, 128.79, 127.03, 126.76, 126.27, 52.63; HRESIMS (LC-MS/MS) Calcd. for $C_{16}H_{14}N_4O_4S$ $[M-H]^+$ 357.0663, found 357.0672.

4.1.3. 4-[3-(Hydrazinocarbonyl)-5-phenyl-1H-1,2,4-triazol-1-yl]-1-benzenesulfonamide **5**

To a stirred solution of ester **4** (3.58 g, 0.01 mol) in ethanol (50 mL), hydrazine monohydrate 98% (2.5 g, 0.05 mol) was added. The mixture was heated at reflux for 6 h, the mixture was cooled to room temperature. The formed precipitate was filtered, dried and recrystallized from ethanol afforded compound **5** as a pale yellow powder; mp: 227–228 °C; Yield = 2.87 g, 80.20%; FT-IR (cm^{-1}): 3362, 3337, 3243, 1655,1598, 1550; ^{1}H NMR (300 MHz, DMSO-d_6) δ 7.84 (d, 2H, J = 8.40 Hz, Ar–H), 7.60 (d, 2H, J = 8.40 Hz, Ar–H), 7.35–7.30 (m, 5H, Ar–H), ^{13}C NMR (75 MHz, DMSO-d_6) 170.10, 155.30, 151.75, 144.01, 142.31, 137.97, 134.10, 127.24, 126.60, 121.29, 114.07; HRESIMS (LC-MS/MS) Calcd. for $C_{15}H_{14}N_6O_3S$ $[M+H]^+$ 359.09209, found 359.09161.

4.1.4. General procedure for synthesis of compounds **6a–d**

To a solution of compound **3** (3.44 g, 0.01 mol) in methanol (30 mL), ammonium hydroxide (25%, 50 mL) or isopropylamine solution (1.18 g, 0.02 mol) or cyclohexylamine (1.98 g, 0.02 mol) or benzylamine (2.14 g, 0.02 mol) was added. The mixture was heated at reflux for 1 h, the solvent was evaporated under reduced pressure, and the formed precipitate was filtered off and recrystallized from ethanol to afford compounds **6a–d**.

4.1.5. 1-[4-(Aminosulfonyl)phenyl]-5-phenyl-1H-1,2,4-triazole-3-carboxamide 6a

Yellow powder; mp: 232–234 °C; Yield = 2.35 g, 68.50%; FT-IR (cm^{-1}): 3478, 3346, 3316, 3225, 1680, 1593, 1547; ^{1}H NMR, 300 MHz, DMSO-d_6, δ ppm: 7.92 (s, 1H, $-SO_2NH$-); 7.89 (s, 1H, $-SO_2NH-$); 7.78–7.74 (m, 4H, Ar–H), 7.57–7.46 (m, 3H, Ar–H), 7.25 (s, 2H, Ar–H), 4.10 (s, 1H, –CONH-); 4.09 (s, 1H, –CONH–); ^{13}C NMR, 100 MHz, DMSO-d_6, δ ppm: 160.24, 156.77, 154.79, 144.59, 139.75, 130.62, 128.96, 128.76, 126.96, 126.88, 126.21; HRESIMS (LC-MS/MS) Calcd. for $C_{15}H_{13}N_5O_3S$ $[M+H]^+$ 344.08119, Found: 344.08078.

4.1.6. N-isopropyl-1-[4-(aminosulfonyl)phenyl]-5-phenyl-1H-1,2,4-triazole-3-carboxamide **6b**

Pale yellow crystals; mp: 236–237 °C; Yield = 2.50 g, 64.90%; ^{1}H NMR, 300 MHz, DMSO-d_6, δ ppm: 8.43 (s, 1H, $-SO_2NH_2$); 8.41 (s, 1H, $-SO_2NH_2$); 7.94 (d, 2H, J = 8.40 Hz, Ar–H), 7.65 (d, 2H, J = 8.40 Hz, Ar–H), 7.56–7.45 (m, 5H, Ar–H), 4.13 (septet, 1H, J = 6.80 Hz, $-C\underline{H}(CH_3)_2$), 1.18 (d, 6H, J = 6.60 Hz, $-CH(\underline{CH_3})_2$); ^{13}C NMR, 75 MHz, DMSO-d_6, δ ppm: 157.65, 156.91, 154.73, 144.68, 139.78, 130.67, 129.02, 128.79, 127.01, 126.91, 126.23, 40.76, 22.09; HRESIMS (LC-MS/MS) Calcd. for $C_{18}H_{19}N_5O_3S$ $[M-H]^+$ 384.11358, Found: 384.11435.

4.1.7. N-cyclohexyl-1-[4-(aminosulfonyl)phenyl]-5-phenyl-1H-1,2,4-triazole-3-carboxamide 6c

Brown powder; mp: 129–130 °C; Yield = 2.72 g, 64%; ^{1}H NMR 300 MHz, DMSO-d_6, δ ppm: 10.50 (bs, 1H, –CONH–), 8.41 (s, 1H, $-SO_2NH_2$); 8.38 (s, 1H, $-SO_2NH_2$); 7.93 (d, 2H, J = 8.40 Hz, Ar–H), 7.64 (d, 2H, J = 8.40 Hz, Ar–H), 7.49–7.45 (m, 5H, Ar–H), 3.82–3.80 (m, 1H, Cyclohexyl-H), 1.70–1.22 (m, 10H, Cyclohexyl-H). ^{13}C NMR, 75 MHz, DMSO-d_6, δ ppm: 157.60, 156.89, 154.73, 144.68, 139.77, 130.66, 129.02, 128.79, 127.34, 126.99, 126.91, 126.23, 48.7, 32.09, 25.11, 24.92, 24.73, 23.92; HRESIMS (LC-MS/MS) Calcd. for $C_{21}H_{23}N_5O_3S$ $[M-H]^+$ 426.15944, Found: 426.15884.

4.1.8. N-Benzyl-1-[4-(aminosulfonyl)phenyl]-5-phenyl-1H-1,2,4-triazole-3-carboxamide **6d**

Pale yellow powder; mp: 138–139 °C; Yield = 2.77 g, 64%; FT-IR (cm^{-1}): 3379, 3330, 3200,1687, 1595, 1547; ^{1}H NMR 300 MHz, DMSO-d_6, δ ppm: 9.29 (t, 1H, J = 6.20 Hz, –CONH–), 8.07 (s, 1H, $-SO_2NH_2$); 8.04 (s, 1H, $-SO_2NH_2$); 7.94 (d, 2H, J = 8.40 Hz, Ar–H), 7.67 (d, 2H, J = 8.40 Hz, Ar–H), 7.56–7.24 (m, 10H, Ar–H); 4.49 (d, 2H, J = 6.20 Hz, –benzylic CH_2); 10.90 (bs, 1H, –CONH–). ^{13}C NMR, 75 MHz, DMSO-d_6: 158.57, 156.68, 154.87, 144.68, 139.75, 139.32, 130.68, 129.49, 129.12, 129.02, 128.83, 128.79, 127.58, 127.40, 126.99, 126.88, 126.83, 126.55, 126.38, 126.23, 120.35, 42.30; HRESIMS (LC-MS/MS) Calcd. for $C_{22}H_{19}N_5O_3S$ $[M+H]^+$ 434.12814, Found: 434.12784.

4.1.9. General procedure for synthesis of compounds **6e–j**

A solution of compound **3** (3.44 g, 0.01 mol) in acetic acid (50 mL), the appropriate aromatic amine (0.01 mol) and anhydrous sodium acetate (1.5 g, 0.018 mol) were added, the mixture was heated under reflux for 3 h. The mixture was cooled to room temperature, poured in ice water (50 mL). The formed precipitate was filtered off, washed with water, dried and recrystallized from ethanol to give compounds **6e–j**.

4.1.10. N-(4-Methylphenyl)-1-[4-(aminosulfonyl)phenyl]-5-phenyl-1H-1,2,4-triazole-3-carboxamide **6e**

Brown powder; mp: 236–238 °C; Yield = 2.68 g, 61.90%; FT-IR (cm^{-1}): 3379, 3330, 3201, 1687, 1595, 1540; ^{1}H NMR 400 MHz, DMSO-d_6, δ ppm: 10.6 (bs, 1H, –CONH–), 8.06 (s, 1H, $-SO_2NH_2$); 7.95 (s, 1H, $-SO_2NH_2$); 7.82–7.70 (m, 5H, Ar–H); 7.60–7.40 (m, 6H, Ar–H), 7.20 (d, 2H, J = 8.20 Hz, Ar–H), 2.30 (s, 3H, CH_3); ^{13}C NMR, 100 MHz, DMSO-d_6: 156.92, 156.78, 154.97, 144.73, 139.67, 135.68, 133.22, 130.74, 129.07, 129.04, 128.79, 126.99, 126.77, 126.30, 120.59, 20.50; HRESIMS (LC-MS/MS) Calcd. for $C_{22}H_{19}N_5O_3S$ $[M+H]^+$ 434.12814, Found: 434.12766.

4.1.11. N-(4-Methoxyphenyl)-1-[4-(aminosulfonyl)phenyl]-5-phenyl-1H-1,2,4-triazole-3-carboxamide **6f**

Dark brown crystals; mp: 210–211 °C; Yield = 3.00 g, 66.80%; FT-IR (cm^{-1}):

3330, 3320, 3211, 1695, 1596, 1533; ^{1}H NMR 400 MHz, DMSO-d_6, δ ppm: 10.5 (bs, 1H, –CONH–), 8.05 (s, 1H, $-SO_2NH_2$); 7.94 (s, 1H, $-SO_2NH_2$); 7.81–7.70 (m, 5H, Ar–H); 7.50–7.42 (m, 6H, Ar–H), 6.95 (d, 2H, J = 8.00 Hz, Ar–H), 3.75 (s, 3H, $-OCH_3$); ^{13}C NMR, 100 MHz, DMSO-d_6: 168.42, 166.67, 156.82, 156.75, 155.87, 144.71, 141.83, 139.69, 138.30, 133.82, 131.25, 130.73, 129.07, 128.79, 128.33, 127.30, 126.99, 126.29, 122.20, 118.64, 113.77, 55.18; HRESIMS (LC-MS/MS) Calcd. for $C_{22}H_{19}N_5O_4S$ $[M+H]^+$ 450.12305, Found: 450.12280.

4.1.12. N-(3,4-Dimethoxyphenyl)-1-[4-(aminosulfonyl)phenyl]-5-phenyl-1H-1,2,4-triazole-3-carboxamide **6g**

Dark brown powder; mp: 235–236 °C; yield = 3.16 g, 66.00%; ^{1}H NMR 300 MHz, DMSO-d_6, δ ppm: 10.39 (s, 1H, –CONH–), 7.97 (s, 1H, $-SO_2NH_2$); 7.95 (s, 1H, $-SO_2NH_2$); 7.71 (d, 2H, J = 8.40 Hz,

Ar–H), 7.57–7.47 (m, 9H, Ar–H); 6.94 (d, 1H, J = 8.40 Hz, Ar–H), 3.75 (s, 3H, $-OCH_3$); 3.74 (s, 3H, $-OCH_3$); ^{13}C NMR, 75 MHz, DMSO-d_6: 156.83, 156.71, 154.98, 148.49, 145.52, 144.76, 139.73, 131.76, 130.77, 129.09, 128.81, 127.02, 126.81, 126.30, 112.52, 111.84, 105.70, 55.72, 55.46; HRESIMS (LC-MS/MS) Calcd. for $C_{23}H_{21}N_5O_5S$ $[M+H]^+$ 478.11906, Found: 478.11957.

4.1.13. N-(4-Chlorophenyl)-1-[4-(aminosulfonyl)phenyl]-5-phenyl-1H-1,2,4-triazole-3-carboxamide **6h**

Buff powder; mp: 268–269 °C; Yield = 2.81 g, 62.00%; ^{1}H NMR 300 MHz, DMSO-d_6, δ ppm: 10.74 (s, 1H, –CONH–), 7.97 (s, 1H, $-SO_2NH_2$); 7.94 (s, 1H, $-SO_2NH_2$); 7.91 (d, 2H, J = 8.40 Hz, Ar–H), 7.71 (d, 2H, J = 8.40 Hz, Ar–H), 7.56–7.41 (m, 9H, Ar–H); ^{13}C NMR, 75 MHz, DMSO-$d6$: 157.19, 156.51, 155.10, 144.81, 139.65, 137.23, 130.78, 129.09, 128.81, 128.56, 127.88, 127.01, 126.73, 126.33, 122.23; HRESIMS (LC-MS/MS) Calcd. for $C_{21}H_{16}ClN_5O_3S$ $[M-H]^+$ 452.05896, Found: 452.05994.

4.2. N-(4-Acetylphenyl)-1-[4-(aminosulfonyl)phenyl]-5-phenyl-1H-1,2,4-triazole-3-carboxamide **6i**

Yellow powder; mp: 215–216 °C; Yield = 3.0 g, 65.10%; ^{1}H NMR 400 MHz, DMSO-d_6, δ ppm: 10.60 (bs, 1H, –CONH–), 8.15 (s, 1H, $-SO_2NH_2$); 8.10 (s, 1H, $-SO_2NH_2$); 8.00–7.92 (m, 5H, Ar H); 7.72 (d, 2H, J = 8.20 Hz, Ar–H), 7.65–7.42 (m, 6H, Ar–H), 2.60 (s, 3H, $-COCH_3$); ^{13}C NMR, 100 MHz, DMSO-d_6: 195.68, 157.42, 156.38, 155.16, 144.82, 142.59, 139.62, 132.45, 130.80, 129.25, 129.10, 128.80, 127.01, 126.67, 126.36, 119.88, 26.50; HRESIMS (LC-MS/MS) Calcd. for $C_{23}H_{19}N_5O_4S$ $[M+H]^+$ 462.12305, Found: 462.12268.

4.2.1. N-(Benzothiazol-2-yl)-1-[4-(aminosulfonyl)phenyl]-5-phenyl-1H-1,2,4-triazole-3-carboxamide **6j**

Yellow powder; mp: 228–229 °C; Yield = 3.04 g, 63.90%; ^{1}H NMR 300 MHz, DMSO-d_6, δ ppm: 12.93 (s, 1H, –CONH–), 8.05 (s, 1H, $-SO_2NH_2$); 8.03 (s, 1H, $-SO_2NH_2$); 7.97 (d, 2H, J = 8.40 Hz, Ar–H), 7.80 (d, 1H, J = 8.40 Hz, Ar–H), 7.73 (d, 2H, J = 8.40 Hz, Ar–H), 7.57–7.33 (m, 8H, Ar–H); ^{13}C NMR, 75 MHz, DMSO-d_6: 158.39, 157.88, 155.33, 155.23, 147.93, 144.88, 139.59, 131.48, 130.90, 129.07, 128.86, 127.04, 126.60, 126.35, 126.20, 123.99, 121.88, 120.51; HRESIMS (LC-MS/MS) Calcd. for $C_{22}H_{16}N_6O_3S_2$ $[M-H]^+$ 475.06525, Found: 475.06598.

4.3. Biology

4.3.1. Screening of the anti-inflammatory activity

The experiments were performed on adult male albino rats, weighing (120–140 g), obtained from the animal house, Minia University. The animals were housed in stainless steel cages, divided into groups of four animals each and deprived of food but not water 24 h before the experiment. The anti-inflammatory activity of the compounds under investigation was studied using carrageenan. A suspension of the tested compounds **4**, **5** and **6a–j**, celecoxib and indomethacin in carboxy methyl cellulose (CMC) solution (0.5% w/v in water) was administered orally in a dose level of (0.28 mmol/kg). Control animals were similarly treated with CMC solution (0.5% w/v in water). After 30 min, 0.1 mL of freshly prepared 1% carrageenan solution in normal saline was injected into the subplantar region of the right hind paw of rats according to the method of Winter et al. An equal volume of saline was injected into the left hind paw of each rat. The right paw thickness was measured by a Vernier celiper (SMIEC) directly before and after 1, 2, 3, 4 and 5 h after carrageenan injection. The anti-inflammatory activity of the tested compounds, celecoxib and indomethacin was calculated as the percentage decrease in edema thickness induced by carrageenan.

4.3.2. Screening of ulcerogenicity

After measuring the anti-inflammatory activity the rats were sacrificed by decapitation. The stomachs were removed, collected, opened along the greater curvature, washed with distilled water and cleaned gently by dipping in saline. The mucosal damage for each stomach was examined with a magnifying lens for the presence of macroscopically visible lesions. The number of lesions in each stomach, if any, was counted and recorded. Ulcers were classified into levels, level I, in which the ulcer area is less than 1 mm^2, level II, in which ulcer area is in the range from 1 to 3 mm^2 and level III, in which the ulcer area more than 3 mm^2 and this rated according to their areas in mm^2.

The data are expressed as mean ± S.E.M, *one way* ANOVA test was applied to determine the significance of the difference between the control group and rats treated with the tested compounds.

4.4. Selectivity to COX-1 and COX-2

COX fluorescent inhibitor screening assay kit (catalog number 700100, Cayman Chemical, Ann Arbor, MI, USA) has been employed to investigate the isozyme-specificity of the synthesized compounds following the procedure suggested by the manufacturer. Briefly, in 96-well plate, either ovine COX-1 or human recombinant COX-2 has been incubated with different concentrations of each tested compound in the presence of the assay buffer (100 mM Tris–HCl, pH 8.0), heme and the fluorometric substrate 10-acetyl-3,7-dihydroxyphenoxazine (ADHP) for 20 min at room temperature. The reaction started after addition of arachidonic acid solution for 2 min at room temperature. Fluorescence of resorufin that is produced by the reaction between PGG2 and the fluorometric substrate were analyzed. DuP-697 (selective COX-2 inhibitor) and SC-560 (selective COX-1 inhibitor) were used as reference compounds. The measured fluorescence intensity is proportional to the amount of produced resorufin, which is proportional to the amount of PGG2 present in each well during the reaction. IC_{50} (μM) which corresponds to the concentration of the inhibitor that causes 50% inhibition of COX-1 or COX-2 activity was calculated from the dose response curve of inhibition (triplicate determinations). Dose-response curves for data conforming to inhibition were fitted to:

$$V_0 = V' - \left[V' \frac{i}{i + (IC_{50})}\right] + V\infty$$

Where: V_0 is the observed rate; i is the concentration of inhibitor I; V' is the observed rate in the absence of inhibitor; V_∞ is the observed rate constant at saturating inhibitor, I; IC_{50} is the concentration that leads to half the maximal change in V_0.

4.5. Docking studies

4.5.1. QSAR modeling

Many molecular descriptors were calculated for each compound employing a calculated molecular properties module according to Girgis et al. [39]. The 2D structures of the training set analogs were imported into the Discovery Studio to calculate various molecular descriptors for each antiinflammotory active agent. The 2D molecular descriptors such as Alog*P*, molecular properties, molecular property counts, and surface area volume were used as input molecular properties that could describe the molecules. Multiple linear regression (MLR) analysis were employed to search for optimal QSAR model that being capable of correlating bioactivity variation across the used training set collection. QSAR models were validated employing leave one-out cross-validation; statistical measures used for the evaluation of model were the number of

compounds in regression N, the regression coefficient r^2. The regression coefficient r^2 is a relative measure of fit by the regression equation. It represents the part of the variation in the observed data that is explained by the regression. The correlation coefficient values closer to 1.0 represent the better fit of the regression. Validation parameter, predictive r^2 (r^2–pred) was calculated for evaluating the predictive capacity of the model, a value of r^2–pred greater than 0.5 indicates the good predictive capacity of the QSAR model. Statistical outliers were identified from experimental versus predicted plots. With regard to QSAR modeling, the first goal was to establish a predictive model with a reasonable number of input features to ensure good generalization performance. While correlating various descriptors with biological activity is the most important means to study structure–activity relationships, the interest lies in deciding when to stop adding a new descriptor to the model. Thus, the optimal model should use the minimum number of descriptors to obtain the best fit. To achieve this, a well accepted method is to find out the saturation point, a point beyond which there is no considerable improvement in the regression coefficient (r^2) values even if a new descriptor is added. MLR technique was used in the present study for selecting a significant set of descriptors in order to build the significant models.

4.5.2. Docking study

The docking analysis was performed using Discovery Studio 2.5 software (Accelrys Inc., San Diego, CA, USA) with fully automated docking tool using "Dockligands (CDOCKER)" protocol running on Dual-core Intel(R) E5300 CPU 2.60 GHz, RAM Memory 2 GB under the Windows XP system. The receptor protein is prepared by deleting water molecules from the protein hierarchy and only protein and its crystal ligand (A heteroatom) are retained. Then hydrogens are added to it and by keeping fixed atom constraints (Tool panel/simulate structures/constraints/create fixed atom constraint) on side chain and backbone of the receptor molecule, only the hydrogens are minimized. The force field applied is CharmM to the receptor and the hydrogens are minimized. After minimization the constraints are removed. The protein is split into the protein part and crystal ligand part. By selecting only the protein part and by clicking on "define selected molecule as receptor" under define and edit binding site sub panel of the Tool panel the protein is defined as receptor molecule. By selecting only the ligand part and clicking on "Define sphere from selection" so that the crystal ligand is used to define the binding site of 15 Å on the receptor molecule. Now the above prepared receptor is given as input for 'input receptor molecule' parameter in the CDOCKER protocol parameter explorer. Ten novel synthesized compounds are sketched in separate windows and saved. Force fields are applied on the molecules and minimized to get lowest energy minimum structure. Each of them is given as input in another parameter meant for 'input ligands' and the protocol were run as many times as the number of inhibitors is selected for the experiment. The various conformations for ligand in this procedure were generated by using molecular dynamics. The generated initial structures for the ligand are further refined using simulated annealing. The CDOCKER energy (-(protein-ligand interaction energies)) of best poses docked into the receptor of all the 10 compounds is calculated and compared with that of interacting residues at active site region with the crystallized inhibitor in the COX-2.

Acknowledgment

The authors thank Dr. Kevin Dalby for providing the laboratory space and advice to T.S.K. financial support for TSK mentor "Dr. Kevin Dalby" was from grants from the National Institute of General Medical Sciences (R01GM059802), the Welch Foundation (F-1390), and Texas Institute for Drug & Diagnostic Development (H-F-0032) for carrying out the selectivity to Cox enzymes.

References

[1] G. Singh, G. Triadafilopoulos, Epidemiology of NSAID induced gastrointestinal complications, J. Rheumatol. (1999) 18–24 (Suppl. 56).
[2] W.L. Smith, D.L. Dewitt, Prostaglandin endoperoxide H synthases-1 and -2, Adv. Immunol. 62 (1996) 167–215.
[3] H.R. Herschman, Prostaglandin synthase 2, Biochim. Biophys. Acta 1299 (1996) 125–140.
[4] A.L. Blobaum, L.J. Marnett, Structural and functional basis of cyclooxygenase inhibition, J. Med. Chem. 50 (2007) 1425–1441.
[5] A.K. Chakraborti, S.K. Garg, R. Kumar, H.F. Motiwala, P.S. Jadhavar, Progress in COX-2 inhibitors: a journey so far, Curr. Med. Chem. 17 (2010) 1563–1593.
[6] R.M. Botting, Cyclooxygenase: Past, present and future, J. Therm. Biol. 31 (2006) 208–219.
[7] J. Naesdal, K. Brown, NSAID-associated adverse effects and acid control aids to prevent them: a review of current treatment options, Drug. Saf. 29 (2006) 119–132.
[8] B. Cryer, NSAID-associated deaths: the rise and fall of NSAID-associated GI mortality, Am. J. Gastroenterol. 100 (2005) 1694–1695.
[9] M. Lazzaroni, P.G. Bianchi, Gastrointestinal side-effects of traditional non-steroidal anti-inflammatory drugs and new formulations, Pharmacol. Ther. 20 (2004) 48–58.
[10] M.W. James, C.J. Hawkey, Assessment of non-steroidal anti-inflammatory drug (NSAID) damage in the human gastrointestinal tract, Br. J. Clin. Pharmacol. 56 (2003) 146–155.
[11] V. Schneider, L.E. Levesque, B. Zhang, T. Hutchinson, J.M. Brophy, Association of selective and conventional nonsteroidal antiinflammatory drugs with acute renal failure: a population-based, nested case-control analysis, Am. J. Epidemiol. 164 (2006) 881–889.
[12] G. Mounier, C. Guy, F. Berthoux, M.N. Beyens, M. Ratrema, M. Ollagnier, Severe renal adverse events with arylcarboxylic non-steroidal anti- inflammatory drugs: results of a eight-year French national survey, Therapie 61 (2006) 255–266.
[13] J. Zadrazil, Nonsteroidal antiinflammatory drugs and the kidney, Vnitr. Lek. 52 (2006) 686–690.
[14] D. Adebayo, I. Bjarnason, Is non-steroidal anti-inflammaory drug (NSAID) enteropathy clinically more important than NSAID gastropathy? Postgrad. Med. J. 82 (2006) 186–191.
[15] J.J. Talley, D.L. Brown, J.S. Carter, M.J. Graneto, C.M. Koboldt, J.L. Masferrer, W.E. Perkins, R.S. Rogers, A.F. Shaffer, Y.Y. Zhang, B.S. Zweifel, K. Seibert, 4-[5-Methyl-3-phenylisoxazol-4-yl]-benzenesulfonamide, Valdecoxib: a potent and selective inhibitor of COX-2, J. Med. Chem. 43 (2000) 775–777.
[16] K. Brune, B. Hinz, Selective cyclooxygenase-2 inhibitors: similarities and differences, Scand. J. Rheumatol. 33 (2004) 1–6.
[17] D.O. Stichtenoth, J.C. Frölich, The second generation of COX-2 inhibitors: what advantages do the newest offer? Drugs 63 (2003) 33–45.
[18] E. Ortiz, J. Manage, Market withdrawal of Vioxx: is it time to rethink the use of COX-2 inhibitors? Care Pharm. 10 (2004) 551–554.
[19] J. Kaur, A. Bhardwaj, S.K. Sharma, F. Wuest, 1,4-Diaryl-substituted triazoles as cyclooxygenase-2 inhibitors: synthesis, biological evaluation and molecular modeling studies, Bioorg. Med. Chem. 21 (2013) 4288–4295.
[20] L. Navidpour, H. Shafaroodi, K. Abdi, M. Amini, M.H. Ghahremani, A.R. Dehpourd, A. Shafieea, Design, synthesis, and biological evaluation of substituted 3-alkylthio-4,5-diaryl-4H-1,2,4-triazoles as selective COX-2 inhibitors, Bioorg. Med. Chem. 14 (2006) 2507–2517.
[21] M. Scholz, A.L. Blobaum, L.J. Marnett, E. Hey-Hawkins, Ortho-carbaborane derivatives of indomethacin as cyclooxygenase (COX)-2 selective inhibitors, Bioorg. Med. Chem. 20 (2012) 4830–4837.
[22] P.N. Praveen Rao, E.E. Knaus, Evolution of nonsteroidal anti-inflammatory drugs (NSAIDs): cyclooxygenase (COX) inhibition and beyond, J. Pharm.Pharm. Sci. 11 (2008) 81s–110s.
[23] M.E. Shoman, M. Abdel-Aziz, O.M. Aly, H.H. Farag, M.A. Morsy, Synthesis and investigation of anti-inflammatory activity and gastric ulcerogenicity of novel nitric oxide-donating pyrazoline derivatives, Eur. J. Med. Chem. 44 (2009) 3068–3076.
[24] El-SM.M.N. Abdel-Hafez, G.A.A. Abuo-Rahma, M. Abdel-Aziz, M.F. Radwan, H.H. Farag, Design, synthesis and biological investigation of certain pyrazole-3-carboxylic acid derivatives as novel carriers for nitric oxide, Bioorg. Med. Chem. 17 (2009) 3829–3837.
[25] G.A.A. Abuo-Rahma, M. Abdel-Aziz, M.A.E. Mourad, H.H. Farag, Synthesis, anti-inflammatory activity and ulcerogenic liability of novel nitric oxide donating/chalcone hybrids, Bioorg. Med. Chem. 20 (2012) 195–206.
[26] M. Abdel-Aziz, G.A.A. Abuo-Rahma, E.A.M. Beshr, T.F.S. Ali, New nitric oxide donating 1,2,4-triazole/oxime hybrids: synthesis, investigation of anti- inflammatory, ulceroginic liability and antiproliferative activities, Bioorg. Med. Chem. 21 (2013) 3839–3849.
[27] G.A.A. Abuo-Rahma, M. Abdel-Aziz, E.A.M. Beshr, T.F.S. Ali, 1,2,4-Triazole/oxime hybrids as new strategy for nitric oxide donors: synthesis, anti- inflammatory, ulceroginicity and antiproliferative activities, Eur. J. Med. Chem. 71 (2014) 185–198.

[28] G.W. Sawdey, Rearrangement of 4-arylazo-2-phenyloxazolin-5-one: a new synthesis of 1H-1,2,4-triazoles, J. Am. Chem. Soc. 79 (1957) 1955–1960.
[29] C.A. Winter, E.A. Risely, G.W. Nuss, Carrageenan- induced edema in hind paw of the rat as an assay for anti-inflammatory drugs, Proc. Soc. Exp. Biol. Med. 111 (1962) 544–547.
[30] S.F. De Andrade, M. Lemosa, E. Comunello, V.F. Noldin, V.C. Filho, R. Niero, Evaluation of the antiulcerogenic activity of *Maytenus robusta* (Celastraceae) in different experimental ulcer models, J. Ethnopharmacol. 113 (2007) 252–257.
[31] M.G. Perrone, P. Vitale, P. Malerba, A. Altomare, R. Rizzi, A. Lavecchia, C. Di Giovanni, E. Novellino, A. Scilimati, Diarylheterocycle core ring features effect in selective COX-1 inhibition, Chem. Med. Chem. 7 (2012) 629–641.
[32] C.J. Smith, Y. Zhang, C.M. Koboldt, J. Muhammad, B.S. Zweifel, A. Shaffer, J.J. Talley, J.L. Masferrer, K. Seibert, P.C. Isakson, Pharmacological analysis of cyclooxygenase-1 in inflammation, Proc. Natl. Acad. Sci. USA 95 (1998) 13313–13318.
[33] J.K. Gierse, S.D. Hauser, D.P. Creely, C. Koboldt, S.H. Rangwala, P.C. Isakson, K. Seibert, Expression and selective inhibition of the constitutive and inducible forms of human cyclo-oxygenase, Biochem. J. 305 (Pt 2) (1995) 479–484.
[34] J.L. Johnson, J. Wimsatt, S.D. Buckel, R.D. Dyer, K.R. Maddipati, Purification and characterization of prostaglandin H synthase-2 from sheep placentalcotyledons, Arch. Biochem. Biophys. 324 (1995) 26–34.
[35] J. Barnett, J. Chow, D. Ives, M. Chiou, R. Mackenzie, E. Osen, B. Nguyen, S. Tsing, C. Bach, J. Freire, et al., Purification, characterization and selective inhibition of human prostaglandin G/H synthase 1 and 2 expressed in the baculovirus system, Biochim. Biophys. Acta 1209 (1994) 130–139.
[36] H. Cao, R. Yu, Y. Tao, D. Nikolic, R.B. van Breemen, Measurement of cyclooxygenase inhibition using liquid chromatography-tandem mass spectrometry, J. Pharm. Biomed. Anal. 54 (2011) 230–235.
[37] R.T. Kroemer, Molecular modelling probes: docking and scoring, Biochem. Soc. Trans. 31 (2003) 980–984.
[38] R.G. Kurumbail, A.M. Stevens, J.K. Gierse, J.J. McDonald, R.A. Stegeman, J.Y. Pak, D. Gildehaus, J.M. Miyashiro, T.D. Penning, K. Seibert, P.C. Isakson, W.C. Stallings, Structural basis for selective inhibition of cyclooxygenase-2 by anti-inflammatory agents, Nature 384 (1996) 644–648.
[39] A.S. Girgis, J. Stawinski, N.S. Ismail, H. Farag, Synthesis and QSAR study of novel cytotoxic spiro[3H-indole-3,2′(1′H)-pyrrolo[3,4-c]pyrrole]-2,3′,5′(1H,2′aH,4′H)-triones, Eur. J. Med. Chem. 47 (2012) 312–322.